

Nonlinearity Estimation in Power Amplifiers Based on Undersampled Temporal Data

Jesús Ibáñez-Díaz, Carlos Pantaleón, Ignacio Santamaría, Tomás Fernández, David Martínez
DICOM, ETSII y Telecom, University of Cantabria
Avda. Los Castros, 39005, Santander, Spain
e-mail: jesus@gtas.dicom.unican.es

Abstract

In this paper we apply undersampling techniques to capture the temporal input-output relationship of RF power amplifiers. This approach avoids the distortion introduced by the upconverter and downconverter stages. We develop polynomial models with memory from the available data and evaluate its performance estimating device parameters like Adjacent power Ratio (ACPR) and AM-AM curves. The estimated parameters show good agreement with the empirical ones.

1. Introduction

Precise and representative power amplifier models are a key factor in order to simulate an entire communication system and essential in order to introduce linearization techniques (e.g., predistortion). This work analyses the distortion caused by power amplifiers driven by wideband signals. The traditional measures (AM-AM and AM-PM curves), characterizations and models (Saleh [1], Poza [2] and Abuelma'atti [3]), which are based on single tone amplitude sweeps are not capable of truly representing the device behavior due to the use of modern wideband digital modulations (OFDM, CDMA, QAM,...) with nonconstant envelope.

Nowadays, analog to digital (A/D) converters have seen significant advances both in performance and speed, while prices have declined. Advances of digital signal processing are evident and the tendency to substitute analog signal processing by their equivalent digital counterpart is widespread. However, the well-known Nyquist limit represents a very serious obstacle preventing the application of DSP techniques at frequencies higher than a few hundreds of MHz.

However, sampling at rates lower than the Nyquist limit, twice the maximum frequency, can still allow for an exact reconstruction of the information content of the

analog signal if the signal is bandpass. This is the undersampling (or bandpass sampling) technique [4-6], that allows exact reconstruction of the original bandpass signal if the sampling rate is at least two times the bandwidth of the signal. An important practical limitation is that the A/D converter (or the Track&Hold) must still be able to effectively operate on the highest frequency component in the signal.

Undersampling is a common technique in several applications, for example, radio receivers using digitization at the intermediate frequency or, in some cases, even at the radio frequency. In this paper we will use this technique for device characterization and develop polynomial models with memory from the available data. Several authors have presented polynomial memoryless models [7], tapped-delay-line models [8], Hammerstein models [9], Volterra models or Neural Network models [10] using input-output temporal measures in order to identify nonlinear systems.

The paper is organized as follows. In Section 2 the data Acquisition System using undersampling is described. In Section 3 several measurements of power amplifiers are presented. Section 4 deals with the polynomial models, and Section 5 presents the main results. Finally, in Section 6, the Conclusions are exposed.

2. Acquisition system

2.1. Undersampling

Bandpass sampling or undersampling consists on sampling a modulated signal using a sampling frequency below the Nyquist rate to achieve frequency translation via intentional aliasing.

An ideal bandpass signal has no frequency components below a certain frequency f_l and above certain frequency f_h . For this bandpass signal, the minimum requirements to

allow for an exact reconstruction are that the sampling rate must be at least two times the bandwidth $f_h - f_l$ of the signal. To ensure that spectrum overlapping does not occur, the sampling frequency f_s must satisfy

$$\frac{2f_h}{k} \leq f_s \leq \frac{2f_l}{k-1} \quad (1)$$

where k is restricted to integer values that satisfy

$$2 \leq k \leq \frac{f_h}{f_h - f_l} \quad (2)$$

and $f_h \leq 2f_l$ (3)

Undersampling reduces drastically the sampling rate (k times), but it has the limitation that the A/D converter must still be able to effectively operate on the highest frequency component of the signal. In addition, stringent requirements on analog bandpass filters could be needed to prevent distortion from noise or signals out of the interest band.

2.2. Acquisition schemes

In the last years, several methods for temporal characterization of power radio frequency (RF) amplifiers have been developed [7,11]. All of them use an acquisition scheme based on the sampling of the demodulated signal at baseband, as the one of the block diagram of Figure 1. In this set-up, a test signal is digitally generated and upconverted to a suitable microwave frequency. The signal must be kept at low level in order to prevent unwanted distortion from the upconverter. Due to the low input signal level, it is necessary to add a low distortion amplifier to be able to observe the saturation characteristics of the power amplifier. A bandpass filter centered at the carrier frequency follows the amplifier and an attenuator is used to minimize the downconverter distortion. Finally, the baseband output signal is sampled at the Nyquist rate.

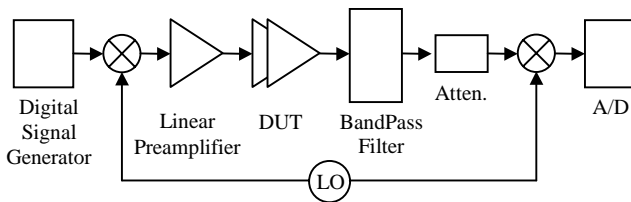


Figure 1: Traditional Measurement Scheme

The main drawback of this scheme is the high linear requirements of the preamplifier and the upconverter and downconverter mixers. In any case, this method is not able to isolating the power amplifier behavior, moreover, it characterizes the whole RF chain (upconversion-amplification-downconversion).

As an alternative, we present a measurement scheme based on the undersampling technique (Figure 2). A digital signal generator generates the test signal, which is upconverted and preamplified in order to drive the RF power amplifier. An exact replica of the input signal, provided by the splitter, is filtered, attenuated (when the signal level is too high) and undersampled by one A/D converter channel. In the same way, the other A/D channel undersamples the DUT output signal after the corresponding filter and attenuator.

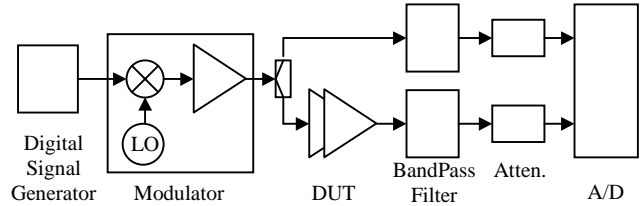


Figure 2: Proposed Measurement Scheme

The HP70820A Transition Analyzer at a rate up to 20 Msps per channel is used to undersample the input and output signal of the Device Under Test. Its large input bandwidth allows the acquisition of signals centered up to 20 GHz with a bandwidth up to 10 MHz.

The use of the digital signal generator, the HP89431 RF modulator (upconversion and preamplification) and the HP70820A (undersampling) provides a great flexibility in RF amplifier characterization. The scheme allows device analysis in any frequency band with any kind of test signal.

The main advantage of this measurement scheme is that it characterizes solely the amplifier behavior, due to the acquisition of the RF input and output signals. Another improvement is the absence of any downconversion stage, avoiding distortion and the hard specifications of traditional measurement schemes. On the other hand, the upconverter and preamplifier distortion become irrelevant, because the real RF power amplifier input signal will be acquired together with the output signal. Finally, this method avoids the problems related with up and down conversion delays and timing errors.

The A/D converter is a critical issue of this undersampling scheme. It must possess sufficient input bandwidth in order to follow the signal highest frequency components (in the carrier frequency band). In the same way, it must provide the adequate sampling rate in order to capture the signal bandpass bandwidth. Nowadays, this last aspect is not restrictive, because commercial A/D converters reach hundreds of megasamples per second, and even a few Gsps. This performance allow us to study the amplifier behavior under high bandwidth driven signals, to relax the bandpass filter specifications and/or to rise the A/D precision trough digital signal processing

techniques (oversampling of the undersampled signal and subsequent decimation).

3. Measurements

The device used in the measurements is the Motorola MRFC1818 GaAs MESFET Power Amplifier working at 1455MHz. Several test signals have been generated in order to extract the amplifier behavior and check the effectiveness of the proposed acquisition and characterization scheme.

In a first approach, we use a coarse representation of an OFDM signal as test signal, consisting on a flat spectrum around a central frequency $f_0 = 5$ MHz with a large number of unitary amplitude carriers having independent random phases with uniform distribution. This results in an amplitude envelope signal following a Rayleigh distribution. A data register of 16000 samples is uploaded to the HP33120A 40 Msps signal generator and periodically repeated at rate of:

$$f_{rep} = 40 \text{ Msps} / 16000 \text{ samples} = 2500 \text{ Hz.} \quad (4)$$

The HP89431 RF section translates the signal to the 1.455 GHz band and performs the preamplification.

A register of 15000 samples per channel is acquired for several input power levels (from -20 dBm to $+5$ dBm). As an example, Figure 3 shows the input and output amplifier power spectrum using a 1 MHz and 0 dBm OFDM type test signal. It is clear the spectral regrowth at the power amplifier output, indicating the nonlinear behavior.

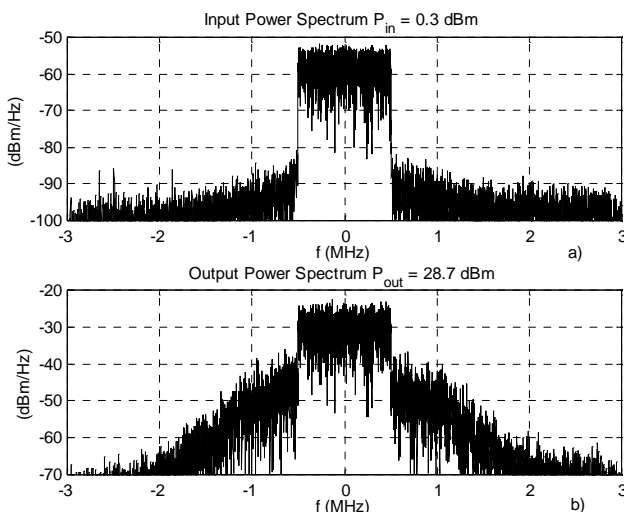


Figure 3: Measured Power Spectrum of an OFDM type signal (BW=1MHz, Pin=0dBm)
a) Input; b) Output

Figure 4 represents the envelope amplitude input-output relationship and clearly shows the saturation effect of the power amplifier for high values of the input.

In the same way, Figure 5 displays the measured input and output envelope amplitude sequences, showing the great significance of the saturation effect in the power amplifier.

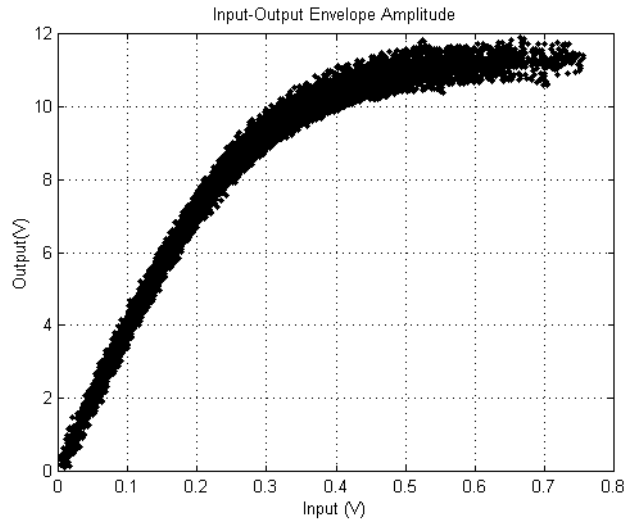


Figure 4: Measured Input-Output Envelope Amplitude of an OFDM type signal (BW=1MHz, Pin=0dBm)

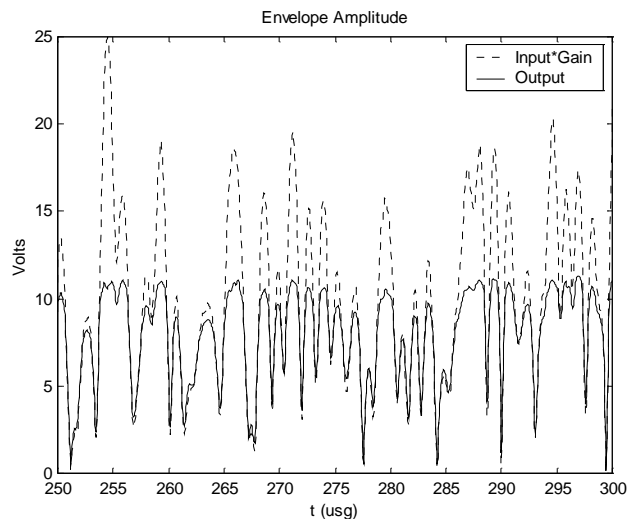


Figure 5: Measured Input and Output Envelope Amplitude signals of an OFDM style signal (BW=1MHz, Pin=0dBm)

Moreover, saturation is not the only remarkable aspect when analyzing the temporal measurements. As Figure 4 shows, the amplifier presents hysteresis, even in the linear region, which suggests some kind of system memory.

Figure 6 shows the relationship between the measured input and output envelope amplitude signals of the amplifier fed with a narrowband DSB-AM signal. The modulating signal is a low frequency (20 KHz) sinusoid, and the modulation deep is 70%. For this input signal, the hysteresis is quite evident.

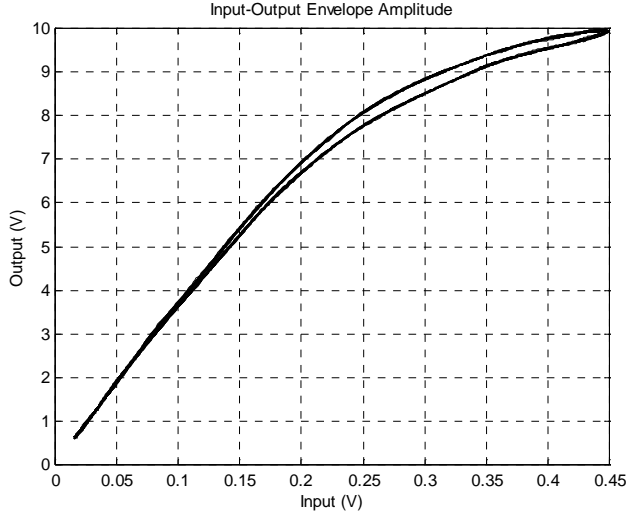


Figure 6: Measured Input-Output Envelope Amplitude of an AM signal

4. Models

Using the available temporal data measurement, we estimate a quadrature nonlinear model similar to the one presented in [12]. A block diagram of the proposed model is shown in Figure 7.

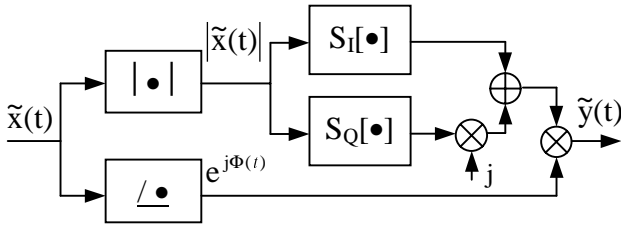


Figure 7: Quadrature Nonlinear Model

The in-phase, $S_I[\cdot]$, and quadrature, $S_Q[\cdot]$, subsystems adjust the output in-phase and quadrature components as a function of the input envelope amplitude. The in-phase and quadrature models have the following input-output relationship

$$\begin{aligned} \tilde{y}_I[n] &= \sum_{k=0}^{L_I} \sum_{j=1}^{N_I} b_{kj}^I |\tilde{x}[n - kn_0]|^j \\ \tilde{y}_Q[n] &= \sum_{k=0}^{L_Q} \sum_{j=1}^{N_Q} b_{kj}^Q |\tilde{x}[n - kn_0]|^j \end{aligned} \quad (5)$$

where L_I and L_Q represents the memory, N_I and N_Q the highest polynomial order and n_0 the distance between the memory taps. Using the amplifier input and output signals the optimum values of b_{kj}^I and b_{kj}^Q are easily calculated by least squares.

An important advantage of this model is its flexibility, since it can represent the simplest AM-AM model, forcing $L_I=0$ and $N_Q=0$; a polynomial memoryless model, with $L_I=L_Q=0$; or a more general model with $L_I=L_Q=L$ and $N_I=N_Q=N$.

5. Results

In this Section we estimate the models of Section 4 from the amplifier measurements obtained in Section 3. Then we simulate some amplifier parameters and compare them with those obtained directly from measurement.

In order to obtain the amplifier model, the first 2000 samples of the temporal acquisitions has been used. The rest of the samples (13000) are used to measure the model accuracy. If we define the estimation error as the mean square error of the difference between the estimated signal, $\hat{y}(t)$, and the measured signal, $\tilde{y}(t)$, then the amplitude estimation error, \hat{e}_A , the in-phase estimation error, \hat{e}_I , and the quadrature estimation error, \hat{e}_Q , can be written as

$$\begin{aligned} \hat{e}_A &= \frac{1}{N} \sum_{n=1}^N (|\tilde{y}[n]| - |\hat{y}[n]|)^2 \\ \hat{e}_I &= \frac{1}{N} \sum_{n=1}^N (\text{Re}\{\tilde{y}[n]\} - \text{Re}\{\hat{y}[n]\})^2 \\ \hat{e}_Q &= \frac{1}{N} \sum_{n=1}^N (\text{Im}\{\tilde{y}[n]\} - \text{Im}\{\hat{y}[n]\})^2 \end{aligned} \quad (6)$$

The estimation signal to noise ratios are thus

$$\begin{aligned} \text{SNR}_A &= \frac{1}{N \cdot \hat{e}_A} \sum_{n=1}^N |\tilde{y}[n]|^2 \\ \text{SNR}_I &= \frac{1}{N \cdot \hat{e}_I} \sum_{n=1}^N \text{Re}\{\tilde{y}[n]\}^2 \\ \text{SNR}_Q &= \frac{1}{N \cdot \hat{e}_Q} \sum_{n=1}^N \text{Im}\{\tilde{y}[n]\}^2 \end{aligned} \quad (7)$$

The MRFC1818 amplifier temporal measurements suggest some kind of memory, which is particularly clear when the amplifier is driven by the AM signal. Table I shows the snr_A obtained by different model parameters.

N	1	2	3	4	5	6	7	8	9	10
L=0	16.3	34.9	35.3	37.2	37.2	37.3	37.3	37.4	37.4	37.4
L=1, n ₀ =100	16.5	38.1	40.6	47.1	47.3	48.4	48.7	49.1	49.0	48.9

Table I: SNR_A (dB) using the AM acquisition.

The Table I clearly shows the superior performance of the one-tap memory models over the memoryless ones. For example there is an improvement of 10 dB between the four order one-tap model ($SNR_A=47.1$, $SNR_I=45.2$, $SNR_Q=45.3$) and the memoryless four order model ($SNR_A=37.2$, $SNR_I=37.1$, $SNR_Q=36.8$).

In order to validate the characterization method based on undersampling, we simulate the adjacent channel power ratio (ACPR) using an amplifier model with $N=10$ and $L=1$ and an OFDM style input signal of 1 MHz of bandwidth and power in the -20 to 10 dBm range. Figure 8 compares the simulation results with the measurements. It shows the measured ACPR at the amplifier input and output and the simulated ACPR. The difference between the simulated and measured output ACPR it is also displayed, showing the great accuracy of the model.

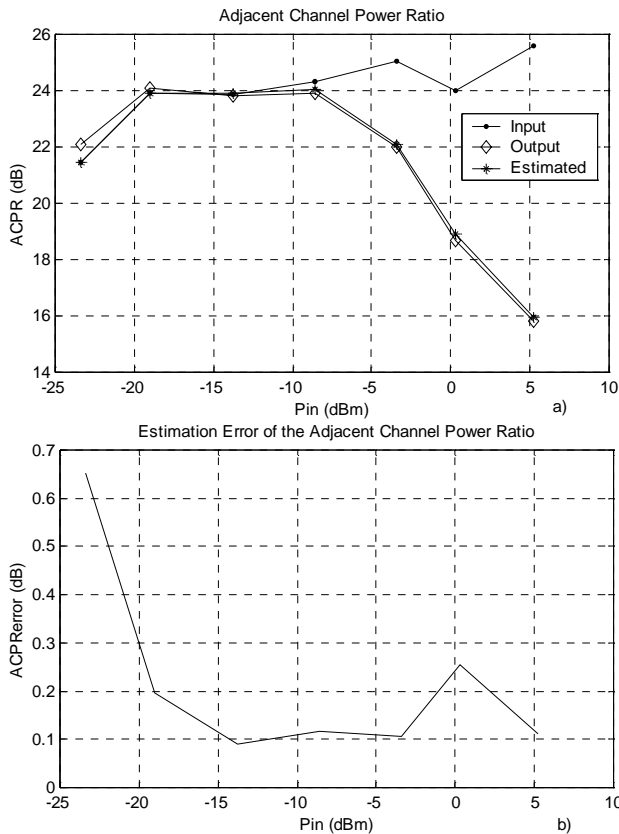


Figure 8: Adjacent Channel Power Ratio. a) Input, Output and Estimated ACPR; b) Estimation Error of the ACPR

Figures 9 and 10 shows the amplitude response of the in-phase and quadrature subsystems of the two taps model. The overall amplitude response of the model, driven with a constant envelope input signal, is presented in Figure 11 and compared with the AM-AM curve

measured with the traditional CW methods. Again, a high agreement is obtained.

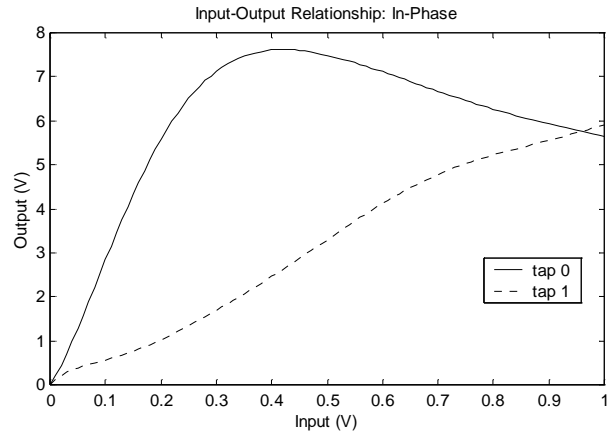


Figure 9: Amplitude Response of the In-phase subsystem model

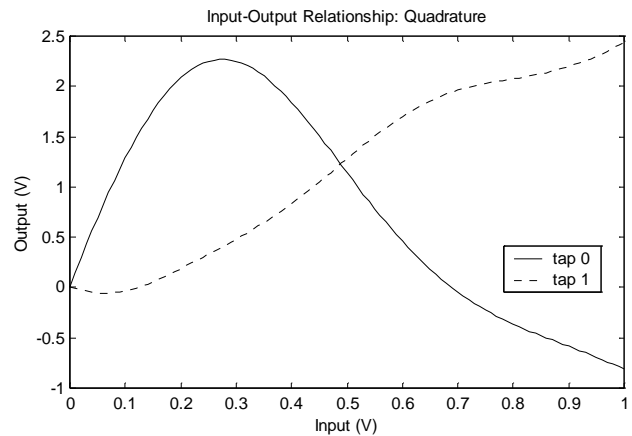


Figure 10: Amplitude Response of the Quadrature subsystem model

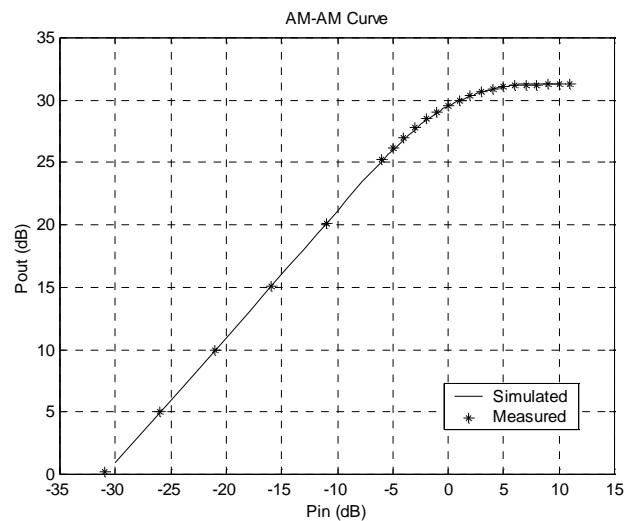


Figure 11: Simulated and Measured AM-AM curve

6. Conclusions

In this paper we have successfully applied undersampling techniques to the characterization of RF power amplifiers. This approach allows characterizing solely the amplifier behavior; avoids the upconverter and preamplifier linearity restrictions; eliminates the downconverter and its distortion; and easily shows the amplifier main characteristics (saturation, hysteresis, memory). The polynomial memory models developed from the acquired data allows obtaining amplifier parameters like ACPR and AM-AM curves that shows good agreement with the empirical measurements. These results validate our undersampling approach.

Further work is been carrying out in order to improve the acquisition scheme. We are using a higher sampling frequency A/D converter that will increase the signal bandwidth and the measurement accuracy. A/D converter characterization is another aspect that will be considered in order to establish its influence on the measurements. Furthermore, this work will allow the development of novel amplifier models and their application on linearization schemes.

References

- [1] A. A. M. Saleh, "Frequency-Independent and Frequency-Dependent Nonlinear Models of TWT Amplifiers", IEEE Trans. on Comm., vol. COM-29, no. 11, pp. 1715-1720, 1981.
- [2] H. B. Poza et all, "A Wideband Data Link Computer Simulation Model", Proc. NAECON Conf., 1975.
- [3] M. T. Abuelma'atti, "Frequency-Dependent Nonlinear Quadrature Model for TWT Amplifiers", IEEE Trans. On Comm., vol. COM-32, no. 8, pp. 982-986, 1984.
- [4] R. G. Vaughan et all, "The Theory of Bandpass Sampling", IEEE Trans. On Signal Processing, vol. 39, no. 9, pp. 1973-1984, 1991.
- [5] G. Hill, "The Benefits of Undersampling", Electronic Design, pp. 69-79, July 11, 1994.
- [6] J. A. Wepman, "Analog-to-Digital Converters and Their Applications in Radio Receivers", IEEE Communications Magazine, pp. 39-45, May 1995.
- [7] V. Borich et all, "Nonlinear Effects of Power Amplification on Multicarrier Spread Spectrum Systems", IEEE MTT-S Digest, pp. 323-326, 1998.
- [8] M. S. Heutmaker et all, "Envelope Distorsion Models with Memory Improve the Prediction of Spectral Regrowth for Some RF Amplifiers", 48th ARFTG Conference Digest, 1996.
- [9] W. Greblicki, "Nonlinearity Estimation in Hammerstein Systems Based on Ordered Observations", IEEE Trans. On Signal Processing, vol. 44, no. 5, pp. 1224-1233, 1996.
- [10] M. Ibnkahla et all, "Neural Network Modeling and Identification of Nonlinear Channels with Memory: Algorithms, Applications asn Analytic Models", IEEE Trans. On Signal processing, vol 46, no. 5, pp. 1208-1220, 1998.
- [11] M. S. Heutmaker, "The error Vector and Power Amplifier Distortion ", IEEE Wireless Comm. Conf., pp. 100-104, 1997.
- [12] M. C. Jeruchim, P. Balaban, K. S. Shanmugan, Simulation of Communication Systems, New York: Plenum Press, 1992, ch 2, pp 141-177.